



## Accurate hybrid techniques for the method of moments in 2D



Sven-Erik Sandström\*, Imad K. Akeab

Department of Physics and Electrical Engineering, Linnaeus University, SE-351 95 Växjö, Sweden

### ARTICLE INFO

#### Article history:

Received 15 September 2014

Accepted 18 December 2015

#### Keywords:

Method of moments

High-order basis functions

Scaling

Sparse matrix

Integration contour

Accurate hybrid method

### ABSTRACT

The integral equations of high frequency electromagnetic scattering can be solved numerically by means of the method of moments. Higher order basis functions such as B-splines is a means to improve the accuracy.

For smooth convex scatterers and high frequencies the oscillatory behaviour of the solution makes it possible to obtain sparse matrices, and some speedup, through modification of the integration path in the integral equation. This is straightforward for the two-dimensional TM case.

In order to increase sparsity and handle the standing waves that are prominent for the TE case, the shadow region can be treated separately, in a hybrid scheme based on *a priori* knowledge about the solution. An accurate method to combine solutions in this hybrid scheme is presented. The hybrid technique reduces the number of basis functions drastically but high accuracy and sparsity are not fully compatible.

© 2016 Elsevier GmbH. All rights reserved.

### 1. Introduction

An object illuminated by an incident electromagnetic wave is a scattering problem that is often treated by means of integral equations. The internal resonances of the object must be handled and higher order basis functions are needed to improve accuracy [1,2]. Since both sparsity and hybrid techniques are implemented, the investigation is restricted to two dimensions here [3].

A sparse version of the method of moments has been developed for the transverse magnetic (TM) case [4,5]. Sparsity was obtained by modifying the integration contour in the integral equation. Scaling, or the use of asymptotic phase [6,7], combined with the properties of the kernel of the integral equation produces sparsity.

In an earlier paper [8], we studied the transverse electric (TE) case. For the TE case, the deep shadow cannot be left out since the fields decay slower than for the TM case. There is also a standing wave pattern in the deep shadow that needs to be resolved. These TE features also appear for 3D problems where the two cases are superimposed to some degree. Sparsity does not lead to a substantial speedup of the computation for the TE case [8].

The present investigation deals with a hybrid scheme that combines a solution that is known *a priori* in the shadow region, with a B-spline expansion in the lit region.

A first objective is to verify that the two solutions can be connected accurately so as to avoid purely numerical phenomena at the matching points. A second objective is to investigate how the use of a hybrid technique affects sparsity and accuracy. A third objective is to find out if the numerical solution is sensitive to the accuracy of the *a priori* solution used in the shadow. A hybrid technique is essentially a divide and conquer strategy and requires that the subproblems can be reasonably well separated.

### 2. The matching problem

As shown in Fig. 1, an incident wave with wavenumber  $k$  impinges on a cylinder that is very long so that the problem can be modelled in two dimensions. Depending on the polarisation of the incident field, either of two integral equations [9, p. 37] for the surface current  $J_s$  on the scatterer is applicable. The extinction theorem [10] and perfectly conducting (PEC) surfaces are used here. In addition, a domain in the shadow, defined by the angle  $\theta_a$  in Fig. 2, is dealt with separately. The simplified 2D problem can then be stated in the form,

$$\begin{aligned} \frac{4}{k} u_i(x, y) &= \int_0^{\theta_a} K_M J_a d\theta' - \int_{2\pi-\theta_a}^{2\pi} K_M J_a d\theta' \\ &= \int_{\theta_a}^{2\pi-\theta_a} H_0^{(1)}(kR) J_s \sqrt{\rho'^2 + \left(\frac{d\rho'}{d\theta'}\right)^2} d\theta', \end{aligned} \quad (1)$$

\* Corresponding author. Tel.: +46 470 708135.

E-mail address: [sven-erik.sandstrom@lnu.se](mailto:sven-erik.sandstrom@lnu.se) (S.-E. Sandström).

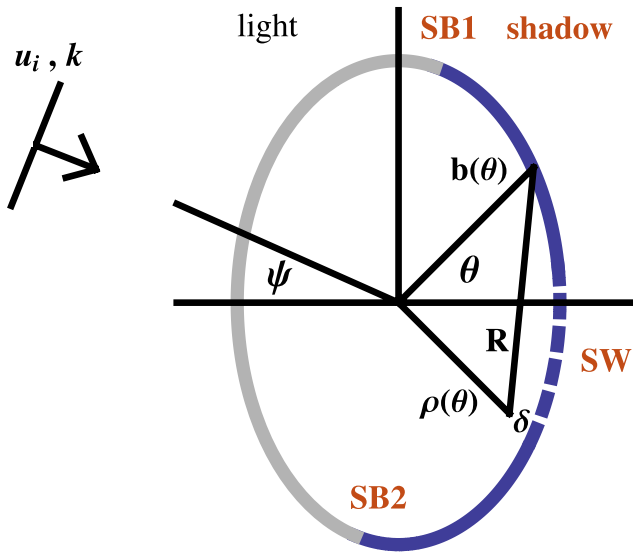


**Fig. 1.** A simple convex 2D geometry where an incident field induces a current on the surface of the scatterer. At high frequencies there is a well-defined shadow region where the current is very small in the deep shadow. For the TE case there is a noticeable standing wave pattern in the deep shadow.

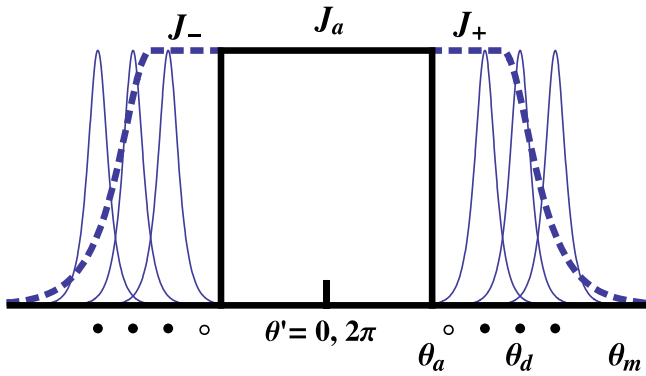


**Fig. 2.** Schematic illustration of the matching of the solution  $J_{a \text{ priori}}$  in the shadow zone and the spline solution in the lit zone. Two smoothly decaying auxiliary functions  $J_+$ ,  $J_-$  are connected to the shadow solution  $J_a$  and combined with the spline solution. The dots at the bottom are observation points. The circles indicate observation points that are not used in the testing.

$$\begin{aligned} \frac{4i}{k} u_i(x, y) - \int_0^{\theta_a} K_E J_a d\theta' - \int_{2\pi-\theta_a}^{2\pi} K_E J_a d\theta' \\ = \int_{\theta_a}^{2\pi-\theta_a} H_1^{(1)}(kR) \hat{R} \cdot \hat{n}' J_s \sqrt{\rho'^2 + \left(\frac{d\rho'}{d\theta'}\right)^2} d\theta'. \end{aligned} \quad (2)$$

$K_M$  and  $K_E$  denote the kernels given in the right hand sides of Eqs. (1) and (2).  $J_a$  is a current that is assumed to be known *a priori* and the corresponding terms are therefore grouped together with the incoming field in this hybrid formulation.  $R$  denotes the distance between the source and the observation point and  $\rho'$  is the radius corresponding to the source point. The boundary is defined by a function  $b(\theta)$  and the radii for the source and the observation points are,

$$\rho'(\theta) = b(\theta), \quad (3)$$

$$\rho(\theta) = b(\theta) - \delta. \quad (4)$$

The parameter  $\delta$  offers a possibility to adjust the smoothness of the kernel of the integral equation. These aspects relate to efficient evaluation of the matrix elements [11,8].

The internal resonances of the scatterer are dealt with by adding the derivative of the equation [10] so as to produce a combined integral equation. Eqs. (1) and (2) are multiplied by a complex factor of order  $k$  and augmented with a regrouped version of the following expressions,

$$\frac{4}{k} \frac{\partial u_i(x, y)}{\partial n} = \int_0^{2\pi} -kH_1 \hat{R} \cdot \hat{n}' J_s \sqrt{\rho'^2 + \left(\frac{d\rho'}{d\theta'}\right)^2} d\theta', \quad (5)$$

$$\begin{aligned} \frac{4i}{k} \frac{\partial u_i(x, y)}{\partial n} = \int_0^{2\pi} \left( \frac{\hat{n} \cdot \hat{n}'}{R} H_1 + \hat{R} \cdot \hat{n}' \hat{R} \cdot \hat{n}' \left( kH_1' - \frac{H_1}{R} \right) \right) \\ \times J_s \sqrt{\rho'^2 + \left(\frac{d\rho'}{d\theta'}\right)^2} d\theta'. \end{aligned} \quad (6)$$

By approximating the surface current  $J_s$  with a set of  $N - 2N_a - p$  basis functions and applying the integral equation at  $N - 2N_a - p$  testing points  $\theta_i$  one obtains a dense linear system of equations for the coefficients  $c_j$  that determine the current.

$$J_s(\theta') = J_a + \sum_{j=N_a}^{N-N_a-p} c_j N_{j,p}(\theta') + J_+ + J_- \quad (7)$$

The *ansatz* for the current  $J_s$  is illustrated schematically in Fig. 2.  $J_a = J_{a \text{ priori}}$  is zero outside the domain defined by  $\theta_a$ . The function  $J_+$  is given by,

$$J_+(\theta') = J_{a \text{ priori}}, \quad (8)$$

if  $\theta_a < \theta' < \theta_d$ . In terms of  $\Delta\theta = \theta' - \theta_d$ ,

$$J_+(\theta') = J_{a \text{ priori}} \sum_{j=0}^M \frac{(c\Delta\theta)^{2j}}{(2j)!} \frac{1}{\cosh c\Delta\theta}, \quad (9)$$

when  $\theta_d < \theta' < \theta_m$ .  $J_+$  is zero elsewhere and  $J_-$  is defined in a similar manner in accordance with Fig. 2.  $J_+$  and  $J_-$  are defined separately from  $J_a$  since they overlap with the spline expansion. Since they are known *a priori* they will also eventually be grouped with the incoming field in Eqs. (1), (2), (5) and (6).

$J_+$  and  $J_-$  must decay smoothly to zero and this is arranged with the function in Eq. (9) that has vanishing derivatives at  $\theta_d$  up to order  $2M$ . The constant  $c$  is adjusted to produce a suitable decay. As shown in Fig. 2, there are only a few splines overlapping close to  $\theta_a$  and  $2\pi - \theta_a$ . To compensate for this,  $J_{\pm}$  has a flat part that essentially eliminates the dependence on the spline solution in the domains where the approximating capacity is poor.

B-splines  $N_{j,p}$  of order  $p$  are used [4,12]. The B-splines are polynomials of order  $p$  with overlapping supports except for  $p=0$ . For a given angle  $\theta'$ , there are then in general  $p+1$  nonzero splines. Fig. 2 shows the case with  $p=2$ . When  $p$  is even, the  $p$  unused testing points can be placed symmetrically, as illustrated by the small circles in the figure.

### 3. Scaling

Earlier work on the TM case [6,4,7] describes an approach that combines the oscillation of the current  $J_s$  and the oscillation of the kernel of the integral equation. The oscillation of the current is factored out,

$$J_s = J_0(\theta') f_{osc}(\theta'). \quad (10)$$

The simple form,

$$f_{osc} = e^{ikb(\theta') \cos(\theta'+\psi)}, \quad (11)$$

Download English Version:

<https://daneshyari.com/en/article/447382>

Download Persian Version:

<https://daneshyari.com/article/447382>

[Daneshyari.com](https://daneshyari.com)